2012

Evidence for Spin Correlation in $t\bar{t}$ Production

V. M. Abazov
Joint Institute for Nuclear Research, Dubna, Russia

Kenneth A. Bloom
University of Nebraska-Lincoln, kenbloom@unl.edu

Daniel R. Claes
University of Nebraska-Lincoln, dclaes@unl.edu

Kayle DeVaughan
University of Nebraska-Lincoln

Aaron Dominguez
University of Nebraska-Lincoln, aarond@unl.edu

See next page for additional authors

Evidence for Spin Correlation in $t\bar{t}$ Production

V. M. Abazov,[34] B. Abbott,[72] B. S. Acharya,[28] M. Adams,[48] T. Adams,[46] G. D. Alexeev,[34] G. Alkhazov,[38] A. Alton,[60,†] G. Alverson,[59] G. A. Alves,[2] M. Aoki,[47] A. Askew,[46] B. Åsman,[40] S. Atkins,[57] O. Atramentov,[64] K. Augsten,[9] C. Avila,[7] J. BackusMayes,[79] F. Badaud,[12] L. Bagby,[47] B. Baldin,[47] D. V. Bandurin,[46] S. Banerjee,[28] E. Barberis,[59] P. Baringer,[55] J. Barreto,[3] J. F. Bartlett,[47] U. Bassler,[17] V. Bazterra,[48] A. Bean,[55] M. Begalli,[3] C. Belanger-Champagne,[40] L. Bellantoni,[47] S. B. Beri,[26] G. Bernardi,[16] R. Bernhard,[21] I. Bertram,[41] M. Besançon,[17] R. Beuselinck,[42] V. A. Bezzubov,[37] P. C. Bhat,[47] V. Bhatnagar,[26] G. Blazey,[49] S. Blessing,[46] K. Bloom,[63] A. Boehnlein,[47] D. Boline,[69] E. E. Boos,[36] G. Borissov,[41] T. Bose,[58] A. Brandt,[75] O. Brandt,[22] R. Brock,[61] G. Brooijmans,[67] A. Bross,[47] D. Brown,[16] J. Brown,[16] X. B. Bu,[47] M. Buehler,[47] V. Buescher,[23] V. Bunichev,[36] S. Burdin,[41,‡] T. H. Burnett,[79] C. P. Buszello,[40] B. Calpas,[14] E. Camacho-Pérez,[31] M. A. Carrasco-Lizarraga,[55] B. C. K. Casey,[47] H. Castilla-Valdez,[31] S. Chakrabarti,[69] D. Chakraborty,[49] K. M. Chan,[53] A. Chandra,[77] E. Chapon,[17] G. Chen,[55] S. Chevalier-Théry,[17] D. K. Cho,[74] S. W. Cho,[30] S. Choi,[30] B. Choudhary,[27] S. Cihangir,[47] D. Claes,[63] J. Clutter,[55] M. Cooke,[47] W. E. Cooper,[47] M. Corcoran,[77] F. Couderc,[17] M.-C. Cousinou,[14] A. Croc,[17] D. Cutts,[74] A. Das,[44] G. Davies,[42] K. De,[75] S. J. de Jong,[33] E. De La Cruz-Burelo,[31] F. Déliot,[17] R. Demina,[68] D. Denisov,[47] S. P. Denisov,[37] S. Desai,[47] C. Deterre,[17] K. DeVaughan,[63] H. T. Diehl,[47] M. Diesburg,[47] P. F. Ding,[43] A. Dominguez,[63] T. Dorland,[79] A. Dubey,[27] L. V. Dudko,[36] D. Duggan,[64] A. Duperrin,[14] S. Dutt,[26] A. Dyshkant,[49] M. Eads,[63] D. Edmunds,[61] J. Ellison,[45] V. D. Elvira,[47] Y. Enari,[16] H. Evans,[51] A. Evdokimov,[70] V. N. Evdokimov,[37] G. Facini,[59] T. Ferbel,[68] F. Fiedler,[23] F. Filthaut,[33] W. Fisher,[61] H. E. Fisk,[47] M. Fortner,[49] H. Fox,[41] S. Fuess,[47] A. Garcia-Bellido,[68] G. A García-Guerra,[31,§] V. Gavrilov,[35] P. Gay,[12] W. Geng,[14,61] D. Gerbaudo,[65] C. E. Gerber,[48] Y. Gershtein,[64] G. Ginther,[47,68] G. Golovanov,[34] A. Goussiou,[79] P. D. Grannis,[69] S. Greder,[18] H. Greenlee,[47] Z. D. Greenwood,[57] E. M. Gregores,[4] G. Grenier,[19] Ph. Gris,[12] J.-F. Grivaz,[15] A. Grohsjean,[17] S. Grünendahl,[47] M. W. Grünewald,[29] T. Guillemin,[15] G. Gutierrez,[47] P. Gutierrez,[72] A. Haas,[67,‖] S. Hagopian,[46] J. Haley,[59] L. Han,[6] K. Harder,[43] A. Harel,[68] J. M. Hauptman,[54] J. Hays,[42] T. Head,[43] T. Hebbeker,[20] D. Hedin,[49] H. Hegab,[73] A. P. Heinson,[45] U. Heintz,[74] C. Hensel,[22] I. Heredia-De La Cruz,[31] K. Herner,[60] G. Hesketh,[43,¶] M. D. Hildreth,[53] R. Hirosky,[78] T. Hoang,[46] J. D. Hobbs,[69] B. Hoeneisen,[11] M. Hohlfeld,[23] Z. Hubacek,[9,17] V. Hynek,[9] I. Iashvili,[66] Y. Ilchenko,[76] R. Illingworth,[47] A. S. Ito,[47] S. Jabeen,[74] M. Jaffré,[15] D. Jamin,[14] A. Jayasinghe,[72] R. Jesik,[42] K. Johns,[44] M. Johnson,[47] A. Jonckheere,[47] P. Jonsson,[42] J. Joshi,[26] A. W. Jung,[47] A. Juste,[39] K. Kaadze,[56] E. Kajfasz,[14] D. Karmanov,[36] P. A. Kasper,[47] I. Katsanos,[63] R. Kehoe,[76] S. Kermiche,[14] N. Khalatyan,[47] A. Khanov,[73] A. Kharchilava,[66] Y. N. Kharzheev,[34] J. M. Kohli,[26] A. V. Kozelov,[37] J. Kraus,[61] S. Kulikov,[37] A. Kumar,[66] A. Kupco,[10] T. Kurča,[19] V. A. Kuzmin,[36] J. Kvita,[8] S. Lammers,[51] G. Landsberg,[74] P. Lebrun,[19] H. S. Lee,[30] S. W. Lee,[54] W. M. Lee,[47] J. Lellouch,[16] L. Li,[45] Q. Z. Li,[47] S. M. Lietti,[5] J. K. Lim,[30] D. Lincoln,[47] J. Linnemann,[61] V. V. Lipaev,[37] R. Lipton,[47] Y. Liu,[6] A. Lobodenko,[38] M. Lokajicek,[10] R. Lopes de Sa,[69] H. J. Lubatti,[79] R. Luna-Garcia,[31,**] A. L. Lyon,[47] A. K. A. Maciel,[2] D. Mackin,[77] R. Madar,[17] R. Magaña-Villalba,[31] S. Malik,[63] V. L. Malyshev,[34] Y. Maravin,[56] J. Martínez-Ortega,[31] R. McCarthy,[69] C. L. McGivern,[55] M. M. Meijer,[33] A. Melnitchouk,[62] D. Menezes,[49] P. G. Mercadante,[4] M. Merkin,[36] A. Meyer,[20] J. Meyer,[22] F. Miconi,[18] N. K. Mondal,[28] G. S. Muanza,[14] M. Mulhearn,[78] E. Nagy,[14] M. Naimuddin,[27] M. Narain,[74] R. Nayyar,[27] H. A. Neal,[60] J. P. Negret,[7] P. Neustroev,[38] S. F. Novaes,[5] T. Nunnemann,[24] G. Obrant,[38,*] J. Orduna,[77] N. Osman,[14] J. Osta,[53] G. J. Otero y Garzón,[1] M. Padilla,[45] A. Pal,[75] N. Parashar,[52] V. Parihar,[74] S. K. Park,[30] R. Partridge,[74,‖] N. Parua,[51] A. Patwa,[70] B. Penning,[47] M. Perfilov,[36] Y. Peters,[43] K. Petridis,[43] G. Petrillo,[68] P. Pétroff,[15] R. Piegaia,[1] M.-A. Pleier,[70] P. L. M. Podesta-Lerma,[31,††] V. M. Podstavkov,[47] P. Polozov,[35] A. V. Popov,[37] M. Prewitt,[77] D. Price,[51] N. Prokopenko,[37] J. Qian,[60] A. Quadt,[22] B. Quinn,[62] M. S. Rangel,[2] K. Ranjan,[27] P. N. Ratoff,[41] I. Razumov,[37] P. Renkel,[76] M. Rijssenbeek,[69] I. Ripp-Baudot,[18] F. Rizatdinova,[73] M. Rominsky,[47] A. Ross,[41] C. Royon,[17] P. Rubinov,[47] R. Ruchti,[53] G. Safronov,[35] G. Sajot,[13] P. Salcido,[49] A. Sánchez-Hernández,[31] M. P. Sanders,[24] B. Sanghi,[47] A. S. Santos,[5] G. Savage,[47] L. Sawyer,[57] T. Scanlon,[42] R. D. Schamberger,[69] Y. Scheglov,[38] H. Schellman,[50] T. Schliephake,[25] S. Schlobohm,[79] C. Schwanenberger,[43] R. Schwienhorst,[61] J. Sekaric,[55] H. Severini,[72] E. Shabalina,[22] V. Shary,[17] A. A. Shchukin,[37] R. K. Shivpuri,[27] V. Simak,[9] V. Sirotenko,[47] P. Skubic,[72] P. Slattery,[68] D. Smirnov,[53] K. J. Smith,[66] G. R. Snow,[63] J. Snow,[71] S. Snyder,[70] S. Söldner-Rembold,[43] L. Sonnenschein,[20] K. Soustruznik,[8] J. Stark,[13] V. Stolin,[35] D. A. Stoyanova,[37] M. Strauss,[72] D. Strom,[48] L. Stutte,[47] L. Suter,[43] P. Svoisky,[72] M. Takahashi,[43] A. Tanasijczuk,[1] M. Titov,[17] V. V. Tokmenin,[34] Y.-T. Tsai,[68] K. Tschann-Grimm,[69] D. Tsybychev,[69] B. Tuchming,[17] C. Tully,[65] L. Uvarov,[38] S. Uvarov,[38] S. Uzunyan,[49] R. Van Kooten,[51] W. M. van Leeuwen,[32] N. Varelas,[48] E. W. Varnes,[44] I. A. Vasilyev,[37] P. Verdier,[19] L. S. Vertogradov,[34] M. Verzocchi,[47] M. Vesterinen,[43] D. Vilanova,[17] P. Vokac,[9] H. D. Wahl,[46]

M. H. L. S. Wang,[47] J. Warchol,[53] G. Watts,[79] M. Wayne,[53] M. Weber,[47,‡‡] L. Welty-Rieger,[50] A. White,[75] D. Wicke,[25] M. R. J. Williams,[41] G. W. Wilson,[55] M. Wobisch,[57] D. R. Wood,[59] T. R. Wyatt,[43] Y. Xie,[47] R. Yamada,[47] W.-C. Yang,[43] T. Yasuda,[47] Y. A. Yatsunenko,[34] Z. Ye,[47] H. Yin,[47] K. Yip,[70] S. W. Youn,[47] J. Yu,[75] T. Zhao,[79] B. Zhou,[60] J. Zhu,[60] M. Zielinski,[68] D. Zieminska,[51] and L. Zivkovic[74]

(D0 Collaboration)

[1]*Universidad de Buenos Aires, Buenos Aires, Argentina*
[2]*LAFEX, Centro Brasileiro de Pesquisas Físicas, Rio de Janeiro, Brazil*
[3]*Universidade do Estado do Rio de Janeiro, Rio de Janeiro, Brazil*
[4]*Universidade Federal do ABC, Santo André, Brazil*
[5]*Instituto de Física Teórica, Universidade Estadual Paulista, São Paulo, Brazil*
[6]*University of Science and Technology of China, Hefei, China*
[7]*Universidad de los Andes, Bogotá, Colombia*
[8]*Charles University, Faculty of Mathematics and Physics, Center for Particle Physics, Prague, Czech Republic*
[9]*Czech Technical University in Prague, Prague, Czech Republic*
[10]*Center for Particle Physics, Institute of Physics, Academy of Sciences of the Czech Republic, Prague, Czech Republic*
[11]*Universidad San Francisco de Quito, Quito, Ecuador*
[12]*LPC, Université Blaise Pascal, CNRS/IN2P3, Clermont, France*
[13]*LPSC, Université Joseph Fourier Grenoble 1, CNRS/IN2P3, Institut National Polytechnique de Grenoble, Grenoble, France*
[14]*CPPM, Aix-Marseille Université, CNRS/IN2P3, Marseille, France*
[15]*LAL, Université Paris-Sud, CNRS/IN2P3, Orsay, France*
[16]*LPNHE, Universités Paris VI and VII, CNRS/IN2P3, Paris, France*
[17]*CEA, Irfu, SPP, Saclay, France*
[18]*IPHC, Université de Strasbourg, CNRS/IN2P3, Strasbourg, France*
[19]*IPNL, Université Lyon 1, CNRS/IN2P3, Villeurbanne, France and Université de Lyon, Lyon, France*
[20]*III. Physikalisches Institut A, RWTH Aachen University, Aachen, Germany*
[21]*Physikalisches Institut, Universität Freiburg, Freiburg, Germany*
[22]*II. Physikalisches Institut, Georg-August-Universität Göttingen, Göttingen, Germany*
[23]*Institut für Physik, Universität Mainz, Mainz, Germany*
[24]*Ludwig-Maximilians-Universität München, München, Germany*
[25]*Fachbereich Physik, Bergische Universität Wuppertal, Wuppertal, Germany*
[26]*Panjab University, Chandigarh, India*
[27]*Delhi University, Delhi, India*
[28]*Tata Institute of Fundamental Research, Mumbai, India*
[29]*University College Dublin, Dublin, Ireland*
[30]*Korea Detector Laboratory, Korea University, Seoul, Korea*
[31]*CINVESTAV, Mexico City, Mexico*
[32]*Nikhef, Science Park, Amsterdam, the Netherlands*
[33]*Radboud University Nijmegen, Nijmegen, The Netherlands and Nikhef, Science Park, Amsterdam, The Netherlands*
[34]*Joint Institute for Nuclear Research, Dubna, Russia*
[35]*Institute for Theoretical and Experimental Physics, Moscow, Russia*
[36]*Moscow State University, Moscow, Russia*
[37]*Institute for High Energy Physics, Protvino, Russia*
[38]*Petersburg Nuclear Physics Institute, St. Petersburg, Russia*
[39]*Institució Catalana de Recerca i Estudis Avançats (ICREA) and Institut de Física d'Altes Energies (IFAE), Barcelona, Spain*
[40]*Stockholm University, Stockholm and Uppsala University, Uppsala, Sweden*
[41]*Lancaster University, Lancaster LA1 4YB, United Kingdom*
[42]*Imperial College London, London SW7 2AZ, United Kingdom*
[43]*The University of Manchester, Manchester M13 9PL, United Kingdom*
[44]*University of Arizona, Tucson, Arizona 85721, USA*
[45]*University of California Riverside, Riverside, California 92521, USA*
[46]*Florida State University, Tallahassee, Florida 32306, USA*
[47]*Fermi National Accelerator Laboratory, Batavia, Illinois 60510, USA*
[48]*University of Illinois at Chicago, Chicago, Illinois 60607, USA*
[49]*Northern Illinois University, DeKalb, Illinois 60115, USA*
[50]*Northwestern University, Evanston, Illinois 60208, USA*
[51]*Indiana University, Bloomington, Indiana 47405, USA*
[52]*Purdue University Calumet, Hammond, Indiana 46323, USA*

[53]University of Notre Dame, Notre Dame, Indiana 46556, USA
[54]Iowa State University, Ames, Iowa 50011, USA
[55]University of Kansas, Lawrence, Kansas 66045, USA
[56]Kansas State University, Manhattan, Kansas 66506, USA
[57]Louisiana Tech University, Ruston, Louisiana 71272, USA
[58]Boston University, Boston, Massachusetts 02215, USA
[59]Northeastern University, Boston, Massachusetts 02115, USA
[60]University of Michigan, Ann Arbor, Michigan 48109, USA
[61]Michigan State University, East Lansing, Michigan 48824, USA
[62]University of Mississippi, University, Mississippi 38677, USA
[63]University of Nebraska, Lincoln, Nebraska 68588, USA
[64]Rutgers University, Piscataway, New Jersey 08855, USA
[65]Princeton University, Princeton, New Jersey 08544, USA
[66]State University of New York, Buffalo, New York 14260, USA
[67]Columbia University, New York, New York 10027, USA
[68]University of Rochester, Rochester, New York 14627, USA
[69]State University of New York, Stony Brook, New York 11794, USA
[70]Brookhaven National Laboratory, Upton, New York 11973, USA
[71]Langston University, Langston, Oklahoma 73050, USA
[72]University of Oklahoma, Norman, Oklahoma 73019, USA
[73]Oklahoma State University, Stillwater, Oklahoma 74078, USA
[74]Brown University, Providence, Rhode Island 02912, USA
[75]University of Texas, Arlington, Texas 76019, USA
[76]Southern Methodist University, Dallas, Texas 75275, USA
[77]Rice University, Houston, Texas 77005, USA
[78]University of Virginia, Charlottesville, Virginia 22901, USA
[79]University of Washington, Seattle, Washington 98195, USA

(Received 20 October 2011; published 19 January 2012)

We present a measurement of the ratio of events with correlated t and $\bar{t}$ spins to the total number of $t\bar{t}$ events. This ratio f is evaluated using a matrix-element-based approach in 729 $t\bar{t}$ candidate events with a single lepton ℓ (electron or muon) and at least four jets. The analyzed $p\bar{p}$ collisions data correspond to an integrated luminosity of 5.3 fb^{-1} and were collected with the D0 detector at the Fermilab Tevatron collider operating at a center-of-mass energy $\sqrt{s} = 1.96$ TeV. Combining this result with a recent measurement of f in dileptonic final states, we find f in agreement with the standard model. In addition, the combination provides evidence for the presence of spin correlation in $t\bar{t}$ events with a significance of more than 3 standard deviations.

DOI: 10.1103/PhysRevLett.108.032004 PACS numbers: 14.65.Ha, 12.38.Qk, 13.85.Qk

Although top and antitop quarks are produced unpolarized at hadron colliders, their spin correlation can be measured, and a significant correlation is expected in the standard model (SM). The strength of spin correlation depends on the production mechanism and differs, for example, for $q\bar{q}$ and gg induced $t\bar{t}$ production [1]. Since the top quark decays through the electroweak interaction before it can interact through the strong interaction [2,3], the spin orientation of the top quark at production is reflected in the angular distributions of the final state particles [4]. We present a measurement of the spin correlation of the t and $\bar{t}$ quarks to check its consistency with that expected in the SM.

The $t\bar{t}$ spin correlation strength C is defined by $d^2\sigma_{t\bar{t}}/(d\cos\theta_1 d\cos\theta_2) = \sigma_{t\bar{t}}(1 - C\cos\theta_1\cos\theta_2)/4$, where $\sigma_{t\bar{t}}$ denotes the $t\bar{t}$ production cross section, and θ_1, θ_2 the angles between the spin-quantization axis and the direction of flight of the down-type fermion from the W boson decay in the respective parent t or $\bar{t}$ rest frame. It is related to the fractional difference $A = (N_a - N_o)/(N_a + N_o)$ in the number of events N_a where the top and antitop quark spins are aligned and those where the top quarks spins have opposite alignment, N_o, by $C = A/|\alpha_1\alpha_2|$ where α_i is the spin analyzing power of the final state fermion under consideration. In next-to-leading-order quantum chromodynamics (NLO QCD) $\alpha_{\ell^+} = 1$ for the charged lepton in $t \to \ell^+\nu_\ell b$ decays and $\alpha_{\bar{d}} = 0.97$ for the antidown quark in $t \to \bar{d}ub$ decays [5]. The value $A = +1$ (-1) corresponds to fully parallel (antiparallel) spins. Using the beam momentum vector as the quantization axis, the SM predicts $A_{\mathrm{SM}} = 0.78^{+0.03}_{-0.04}$ at NLO QCD for $p\bar{p}$ collisions at $\sqrt{s} = 1.96$ TeV [4].

Three $t\bar{t}$ spin correlation measurements based on the double differential angular distribution have been published so far [6–8]. However, none of them had sufficient sensitivity to distinguish between the hypothesis of spin

correlation, as predicted by the SM, and no spin correlation. A fourth measurement was performed by the D0 Collaboration in an analysis of 5.4 fb^{-1} of integrated luminosity in the $t\bar{t}$ dilepton channel, and reached an expected sensitivity of 3 standard deviations (SDs) from the no-correlation hypothesis. In that analysis [9], leading-order (LO) matrix elements (MEs) were used to measure the ratio f of events with correlated t and $\bar{t}$ spins to the total number of $t\bar{t}$ events by comparing Monte Carlo (MC) simulations with SM spin correlation and without spin correlation to data.

In this Letter, we present the first measurement of the ratio f using the matrix-element approach in $t\bar{t}$ ℓ + jets events. The t and $\bar{t}$ quarks are each assumed to decay into a W boson and a b quark, with one of the W bosons decaying directly or via a leptonic tau decay into an electron or muon and the corresponding neutrinos and the other W boson decaying into two quarks. We use 5.3 fb^{-1} of integrated luminosity collected with the D0 detector at the Fermilab Tevatron $p\bar{p}$ collider and combine our results with the corresponding measurement in the dilepton channel [9].

A description of the D0 detector can be found elsewhere [10]. We use the same event selections as in the measurement of $\sigma_{t\bar{t}}$ in the ℓ + jets channel [11]. We require one isolated electron with transverse momentum $p_T > 20$ GeV and pseudorapidity $|\eta| < 1.1$ [12], or one isolated muon with $p_T > 20$ GeV and $|\eta| < 2.0$, as well as an imbalance in transverse momentum $\not{p}_T > 20(25)$ GeV for the e + jets (μ + jets) channel. Events containing two isolated charged leptons with $p_T > 15$ GeV are rejected, to avoid overlap with the dilepton channel. In addition, we require at least four jets reconstructed using a midpoint cone algorithm [13] with radius $\mathcal{R} = 0.5$, $p_T > 20$ GeV, and $|\eta| < 2.5$; the jet with largest transverse momentum must have $p_T >$ 40 GeV. Jets originating from b quarks are identified using the output of a neural network where variables characterizing the properties of secondary vertices and tracks with large impact parameters relative to the $p\bar{p}$ interaction vertex are combined [14].

The $t\bar{t}$ signal, with contributions from both $q\bar{q} \to t\bar{t}$ and $gg \to t\bar{t}$, is modeled using the MC@NLO [15] event generator with the CTEQ6M1 parton distribution functions (PDFs) [16], assuming a top quark mass $m_t = 172.5$ GeV. We generate $t\bar{t}$ MC samples both with and without the expected spin correlation, corresponding to $A = 0.78$ and $A = 0$, respectively [17]. The events are further processed through HERWIG [18] to simulate parton evolution, hadronization, and decays of short-lived particles, followed by a full detector simulation using GEANT [19]. We overlay events from random beam crossings on the MC events to model the effects of detector noise and additional $p\bar{p}$ interactions. The same reconstruction programs are used to process the data and the simulated events.

The background can be split into two components: multijet background, where some of the products of hadronic partons are misreconstructed as an isolated lepton, and inherent background from SM processes with final states similar to that of the $t\bar{t}$ signal. In the e + jets channel, background from multijet production arises mainly when a jet with high electromagnetic content mimics an electron. In the μ + jets channel it occurs primarily when a muon originates from the decay of a heavy-flavor quark (b or c) and appears to be isolated. The multijet background is estimated from data [11]. The SM background is predominantly from W + jets production, with smaller contributions arising from single top quark, diboson (WW, WZ and ZZ), and Z + jets ($Z \to ee$ in e + jets or $Z \to \mu\mu$ in μ + jets as well as $Z \to \tau\tau$) events. The W + jets contribution is normalized to data using an iterative procedure, where the expected $t\bar{t}$ and smaller SM background contributions are subtracted from the data before application of b-jet tagging [11]. The differential distributions for W + jets are taken from a simulation using the ALPGEN MC program [20]. All smaller SM background contributions are also estimated using MC simulations but normalized to their next-to-leading-order predictions. Diboson events are generated with PYTHIA [21], single top quark production with the COMPHEP generator [22], and Z + jets events are simulated using ALPGEN. All MC background samples are generated using the CTEQ6L1 PDF [16]. The evolution of partons and the hadronization process are simulated using PYTHIA. A matching scheme is applied to avoid double counting of partonic event configurations [23].

To make optimal use of the kinematic information in $t\bar{t}$ events, we calculate signal probabilities P_{sgn} for each event using the LO ME for the hypothesis of correlated ($H = c$) top quark spins, as predicted by the SM for $q\bar{q} \to t\bar{t}$, and for the hypothesis of uncorrelated ($H = u$) spins [1,24]. We can write P_{sgn} as a function of the hypotheses $H = c$ and $H = u$ as:

$$P_{\text{sgn}}(x; H) = \frac{1}{\sigma_{\text{obs}}} \int f_{\text{PDF}}(q_1) f_{\text{PDF}}(q_2) dq_1 dq_2 \times \frac{(2\pi)^4 |\mathcal{M}(y, H)|^2}{q_1 q_2 s} W(x, y) d\Phi_6, \quad (1)$$

with σ_{obs} being the LO $q\bar{q} \to t\bar{t}$ production cross section including selection efficiency and acceptance effects, q_1 and q_2 denoting the fraction of the proton and antiproton momentum carried by the partons, f_{PDF} representing the parton distribution functions, s the square of the center-of-mass energy of the colliding $p\bar{p}$ system, and $d\Phi_6$ the infinitesimal volume element of the six-body phase space. Detector resolution effects are taken into account by introducing transfer functions $W(x, y)$ that describe the probability of a partonic final state y to be measured as $x = (\tilde{p}_1, \ldots, \tilde{p}_n)$, where $\tilde{p}_i$ denote the measured four-momenta of the final state objects (leptons and jets). For the hypothesis $H = c$, we use the ME for the full process $q\bar{q} \to t\bar{t} \to W^+ b W^- \bar{b} \to \ell^+ \nu_\ell b q \bar{q}' \bar{b}$ [25] averaged over the color and spins of the initial partons, and summed over the final

colors and spins [1]. For the hypothesis $H = u$, we use the ME for the same process, neglecting the spin correlation. The total $t\bar{t}$ production cross section $\sigma_{t\bar{t}}$ and the selection efficiency do not depend on spin correlation, thus the normalization factor σ_{obs} can be omitted in Eq. (1). To reduce the number of dimensions for the integrals, we assume the directions of the momenta of jets and charged leptons, and the electron energy are all well measured, and that the $t\bar{t}$ system has negligible transverse momentum. In addition, we use the known masses of the final state particles as constraints.

As we use only four jets when calculating P_{sgn}, there are 24 possible jet-parton assignments. This further can be reduced to four when identifying the jets originating from b quarks. If more than two jets are b tagged, we select only the two jets with the largest b-tag neural network probability as the b jets, and assume other jets to be light-flavor jets. Given the inability to distinguish the flavor of the two quarks from the W decay, as required for the definition of the spin correlation variable, both possible jet-parton assignments have to be considered in the P_{sgn} calculation. Additional details of the P_{sgn} calculation can be found in Ref. [26].

To distinguish between correlated and uncorrelated top quark spin hypotheses, we define, as in Ref. [9], a discriminant R [27],

$$R = \frac{P_{\text{sgn}}(x; H = c)}{P_{\text{sgn}}(x; H = u) + P_{\text{sgn}}(x; H = c)}. \quad (2)$$

To measure the ratio f_{meas} of events with correlated spins to the total number of events, we form templates from distributions of R for $t\bar{t}$ MC events with and without spin correlation as well as background. Since the main sources of background are from multijet and W + jets events, P_{sgn} is only calculated for these two contributions. The smaller backgrounds are modeled using the templates for W + jets production. The templates are compared to the distribution of R in the data, and the fraction f_{meas} is extracted through a binned maximum-likelihood fit. To minimize the dependence of the result on absolute normalization, we calculate the predicted number of events as a function of f_{meas} and $\sigma_{t\bar{t}}$, and extract both simultaneously. Events used in the templates are required to have at least two b-jet candidates; nonetheless, events with fewer than two b-tagged jets are included in the fit to constrain the signal and background normalization. The fitting procedure and b-jet identification criteria are the same as used in Ref. [28].

To enhance the sensitivity, we divide events into four subsamples as a correct jet-to-parton assignment greatly improves the discrimination power of R. The events are divided into two groups of events with exactly four jets and more than four jets to reduce the dilution from initial and final state radiation. To reduce the contamination from events in which a b quark jet is mistakenly taken to come from a W boson decay, these two groups are again separated according to whether the invariant mass of the two light-flavor jets is within or outside of ± 25 GeV of the W boson mass. The ± 25 GeV window is based on optimization through pseudoexperiments. The main sensitivity to spin correlation is obtained in the subsample with four jets and a dijet invariant mass close to the W boson mass, where the probability of selecting the correct jet combination is the highest. In Fig. 1, the measured discriminant R for the most sensitive sample is compared for data and templates of $t\bar{t}$ production with SM spin correlation and without spin correlation, including background.

We consider the same systematic uncertainties as used in the measurement of the $t\bar{t}$ production cross section [11] and $t\bar{t}$ spin correlation in dilepton events [9]. These are included in the likelihood fit through free parameters, where each independent source of systematic uncertainty is modeled as a Gaussian probability density function with zero mean and an rms corresponding to one SD in the uncertainty on that parameter. Correlations among systematic uncertainties for different channels are taken into account by using a single parameter to represent the same source of uncertainty.

We distinguish between systematic uncertainties that affect the yield of the signal or background and those that change the distribution of R. We consider the jet energy scale, b-jet energy scale, jet energy resolution, jet identification, b-tagging efficiency and b-jet misidentification rate, choice of PDF, and the choice of m_t in the calculation of P_{sgn} as the uncertainties that affect the distribution of R. Systematic uncertainties on normalizations include those on lepton identification, trigger

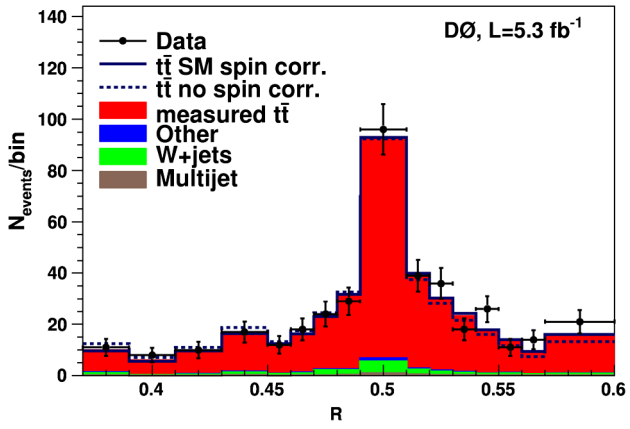

FIG. 1 (color online). The distribution of the discriminant R for ℓ + jets events with four jets and an invariant mass of the two light-flavor jets within ± 25 GeV of the mass of the W boson. The expectation (including background) for complete spin correlation as predicted by the SM ($f = 1$) and the case of no spin correlation ($f = 0$), as well as the $t\bar{t}$ contribution for f_{meas}, where f_{meas} was taken from the combined fit in the ℓ + jets and dilepton final states, are shown. The first and last bins include contributions from $R < 0.37$ and $R > 0.60$, respectively. The bin width is chosen to minimize the statistical uncertainty.

TABLE I. Summary of uncertainties on f_{meas} for the combined fit in dilepton and ℓ + jets channels.

Source	+1SD	−1SD
Muon identification	0.003	−0.003
Electron identification and smearing	0.009	−0.008
PDF	0.058	−0.051
m_t	0.024	−0.040
Triggers	0.007	−0.008
Opposite charge selection	0.002	−0.002
Jet energy scale	0.005	−0.028
Jet reconstruction and identification	0.007	−0.035
b tagging	0.012	−0.012
Normalization	0.039	−0.043
MC statistics	0.015	−0.015
Instrumental background	0.003	−0.003
Luminosity	0.023	−0.023
Multijet background	0.007	−0.007
Other	0.007	−0.007
MC statistics for template fits	0.156	−0.156
Total systematic uncertainty	0.176	−0.184
Statistical uncertainty	0.251	−0.258

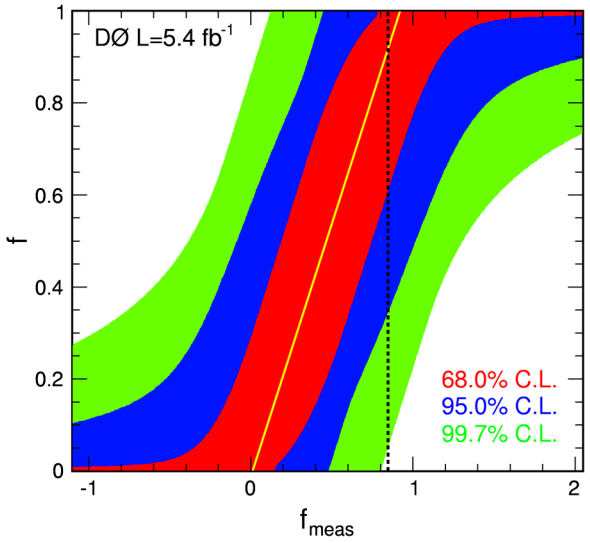

FIG. 2 (color online). Bands for 68%, 95% and 99.7% C.L. of f as a function of f_{meas} for the combined dilepton and ℓ + jets fit. The thin light-color line indicates the most probable value of f as a function of f_{meas}. The vertical dotted black line shows the measured value of $f_{\text{meas}} = 0.85$.

requirements, the normalization of background, the luminosity, MC modeling, and the determination of multijet background. We also include an uncertainty on the shape of the templates varying each template bin within its statistical uncertainty.

MC pseudoexperiments for different values of f are used to estimate the expected uncertainty on f_{meas}, based on the maximum-likelihood fits that provide the dependence of f on f_{meas}. The ordering principle for ratios of likelihoods [29] is applied to the distributions of f and f_{meas}, without constraining f_{meas} to the physically allowed region. From a total of 729 events in the ℓ + jets channels with a $t\bar{t}$ signal purity of 90%, we obtain $f_{\text{meas}} = 1.15^{+0.42}_{-0.43}(\text{stat} + \text{syst})$ and can exclude values of $f < 0.420$ at the 95% C.L. Since the samples of dilepton [9] and ℓ + jets final states are statistically independent, results from the two channels can be combined by adding the logarithms of the likelihood functions and repeating the maximum-likelihood fit. We obtain

$$f_{\text{meas}} = 0.85 \pm 0.29(\text{stat} + \text{syst}) \quad (3)$$

and a $t\bar{t}$ production cross section of $\sigma_{t\bar{t}} = 8.17^{+0.78}_{-0.67}$ pb, which is in good agreement with the SM prediction [30] and previous measurements [11]. The statistical and systematic uncertainties on f_{meas} are given in Table I. For an expected fraction of $f = 1$, we can exclude $f < 0.481$ at the 95% C.L. For the observed value of $f_{\text{meas}} = 0.85$, we can exclude $f < 0.344$ (0.052) at the 95 (99.7)% C.L. We therefore obtain first evidence of SM spin correlation at 3.1 standard deviations. The probability to have a true value of $f = 0$ for the observed value of $f_{\text{meas}} = 0.85$ is 0.16%. Figure 2 shows corresponding bands of confidence level.

The ratio f_{meas} can be used to obtain a measurement of the fractional difference A_{meas} by applying it as a multiplicative factor to the NLO QCD prediction of A_{SM}: $A_{\text{meas}} = f_{\text{meas}} A_{\text{SM}}$. This yields $A_{\text{meas}} = 0.66 \pm 0.23(\text{stat} + \text{syst})$ [31].

In conclusion, we have presented the first measurement of $t\bar{t}$ spin correlation using a matrix-element-based approach in the ℓ + jets channel. When combined with our previous result in the dilepton channel, we obtain significant evidence for the presence of spin correlation in $t\bar{t}$ events with 3.1 standard deviations.

We thank the staffs at Fermilab and collaborating institutions, and acknowledge support from the DOE and NSF (USA); CEA and CNRS/IN2P3 (France); FASI, Rosatom, and RFBR (Russia); CNPq, FAPERJ, FAPESP, and FUNDUNESP (Brazil); DAE and DST (India); Colciencias (Colombia); CONACyT (Mexico); KRF and KOSEF (Korea); CONICET and UBACyT (Argentina); FOM (The Netherlands); STFC and the Royal Society (United Kingdom); MSMT and GACR (Czech Republic); CRC Program and NSERC (Canada); BMBF and DFG (Germany); SFI (Ireland); The Swedish Research Council (Sweden); and CAS and CNSF (China).

*Deceased.
†Visitor from Augustana College, Sioux Falls, SD, USA.
‡Visitor from The University of Liverpool, Liverpool, UK.
§Visitor from UPIITA-IPN, Mexico City, Mexico.
‖Visitor from SLAC, Menlo Park, CA, USA.
¶Visitor from University College London, London, UK.

[**]Visitor from Centro de Investigacion en Computacion—IPN, Mexico City, Mexico.
[††]Visitor from ECFM, Universidad Autonoma de Sinaloa, Culiacán, Mexico.
[‡‡]Visitor from Universität Bern, Bern, Switzerland.

[1] G. Mahlon and S. Parke, Phys. Rev. D **53**, 4886 (1996); G. Mahlon and S. Parke, Phys. Lett. B **411**, 173 (1997).
[2] I. Bigi, Y. Dokshitzer, V. Khoze, J. Kühn, and P. Zerwas, Phys. Lett. B **181**, 157 (1986).
[3] V. M. Abazov *et al.* (D0 Collaboration), Phys. Rev. Lett. **106**, 022001 (2011).
[4] W. Bernreuther, A. Brandenburg, Z. G. Si, and P. Uwer, Nucl. Phys. B **690**, 81 (2004).
[5] A. Brandenburg, Z. G. Si, and P. Uwer, Phys. Lett. B **539**, 235 (2002).
[6] B. Abbott *et al.* (D0 Collaboration), Phys. Rev. Lett. **85**, 256 (2000).
[7] T. Aaltonen *et al.* (CDF Collaboration), Phys. Rev. D **83**, 031104(R) (2011).
[8] V. M. Abazov *et al.* (D0 Collaboration), Phys. Lett. B **702**, 16 (2011).
[9] V. M. Abazov *et al.* (D0 Collaboration), Phys. Rev. Lett. **107**, 032001 (2011).
[10] V. M. Abazov *et al.* (D0 Collaboration), Nucl. Instrum. Methods Phys. Res., Sect. A **565**, 463 (2006).
[11] V. M. Abazov *et al.* (D0 Collaboration), Phys. Rev. D **84**, 012008 (2011).
[12] The pseudorapidity η is defined relative to the center of the detector as $\eta = -\ln[\tan(\theta/2)]$ where θ is the polar angle with respect to the proton beam direction.
[13] G. C. Blazey *et al.*, arXiv:hep-ex/0005012.
[14] V. M. Abazov *et al.* (D0 Collaboration), Nucl. Instrum. Methods Phys. Res., Sect. A **620**, 490 (2010).
[15] S. Frixione and B. R. Webber, J. High Energy Phys. 06 (2002) 029.
[16] J. Pumplin *et al.* (CTEQ Collaboration), J. High Energy Phys. 07 (2002) 012.
[17] In MC@NLO the top quark decays are simulated in LO QCD. We have checked that the difference between the spin analyzing power $\alpha_{\bar{d}}$ in LO and NLO QCD does not impact the final numerical result of A_{meas}.
[18] G. Corcella *et al.*, J. High Energy Phys. 01 (2001) 010.
[19] R. Brun and F. Carminati, CERN Program Library Long Writeup Report No. W5013, 1993 (unpublished).
[20] M. L. Mangano *et al.*, J. High Energy Phys. 07 (2003) 001.
[21] T. Sjöstrand *et al.*, Comput. Phys. Commun. **135**, 238 (2001).
[22] E. Boos *et al.* (CompHEP Collaboration), Nucl. Instrum. Methods Phys. Res., Sect. A **534**, 250 (2004).
[23] M. L. Mangano, M. Moretti, F. Piccinini, and M. Treccani, J. High Energy Phys. 01 (2007) 013.
[24] We do not use MEs for the smaller $gg \to t\bar{t}$ contribution in the calculation of P_{sgn}, but account for it in the measurement by using NLO $t\bar{t}$ MC simulations with $q\bar{q}$ and gg production to extract f.
[25] Throughout this Letter, charge conjugated processes are included implicitly.
[26] F. Fiedler *et al.*, Nucl. Instrum. Methods Phys. Res., Sect. A **624**, 203 (2010).
[27] K. Melnikov and M. Schulze, Phys. Lett. B **700**, 17 (2011).
[28] V. M. Abazov *et al.* (D0 Collaboration), Phys. Rev. D **83**, 092002 (2011).
[29] G. J. Feldman and R. D. Cousins, Phys. Rev. D **57**, 3873 (1998).
[30] S. Moch and P. Uwer, Phys. Rev. D **78**, 034003 (2008); U. Langenfeld, S. Moch, and P. Uwer, Phys. Rev. D **80**, 054009 (2009); M. Aliev *et al.*, Comput. Phys. Commun. **182**, 1034 (2011).
[31] It should be noted that the allowed region for f is restricted to $0 \leq f \leq 1$, resulting in the constraint $0 \leq A \leq 1$, while in principle A can assume any value between -1 and 1. Therefore, values of A derived from f can be compared to direct measurements of A only when assuming that A has a positive value, between 0 and the SM value.